Electrical Power and Energy Systems 54 (2014) 650–657

Contents lists available at ScienceDirect

Electrical Power and Energy Systems

journal homepage: www.elsevier.com/locate/ijepes

# A simplified nonlinear controller for transient stability enhancement of multimachine power systems using SSSC device

Jean de Dieu Nguimfack-Ndongmo [a], Godpromesse Kenné [a,*], René Kuate-Fochie [a], André Cheukem [a], Hilaire Bertrand Fotsin [b], Françoise Lamnabhi-Lagarrigue [c]

[a] Laboratoire d'Automatique et d'Informatique Appliquée (LAIA), Département de Génie Électrique, IUT FOTSO Victor Bandjoun, Université de Dschang, B.P. 134 Bandjoun, Cameroon
[b] Laboratoire d'Electronique, d'Electrotechnique et d'Automatique (LEEA), Département de Physique, Faculté des Sciences, Université de Dschang, Cameroon
[c] Laboratoire des Signaux et Systèmes (LSS), CNRS, Université de Paris XI, 91192 Gif-Sur-Yvette, France

ARTICLE INFO

*Article history:*
Received 22 August 2012
Received in revised form 26 July 2013
Accepted 22 August 2013

*Keywords:*
Power system
Transient stability
FACTS
SSSC
DFIG
Lyapunov theory

ABSTRACT

In this paper, a simplified nonlinear method is proposed to enhance the transient stability of multimachine power system by using a Static Synchronous Series Compensator (SSSC). The rate of dissipation of transient energy is used to determine the additional damping provided by a SSSC. The proposed algorithm is based on the direct Lyapunov method. The simplicity of the proposed scheme and its robustness with respect to large disturbances constitute the main positive features. Simulation results in the case of 3-machines power system show the effectiveness of the proposed method under large disturbances (3-phase and single phase short-circuits).

© 2013 Elsevier Ltd. All rights reserved.

## 1. Introduction

### 1.1. Antecedents and motivations

The fast development of the power electronics industry has permitted the use of Flexible AC Transmission Systems (FACTS) controllers in power systems. The potential benefits with the utilization of FACTS devices include reduction of operation and transmission investment costs, increasing system security and reliability, and increasing transfer capabilities in a deregulated environment [1]. The detailed explanations about the FACTS controllers are well documented in the literature and can be found in [2–4]. Static synchronous series compensator (SSSC) is one of the important type of FACTS family which can be installed in series in the transmission lines. SSSC is very effective in controlling power flow in a transmission line with the capability to change its reactance characteristic from capacitive to inductive [4–6]. An auxiliary stabilizing signal can also be superimposed on the power flow control function of the SSSC to improve power system stability [7]. In [7], the author proposed a SSSC damping controller based on phase compensation for single-machine infinite-bus and an objective function based searching algorithm is suggested for multimachine power system. Menniti et al. [8] proposed the use of SSSC to damp the transient frequency deviation in a deregulated electric power system. This method is based on the application of the overlapping decomposition technique to design a decentralized control law of a SSSC device where a multi-area power system is decomposed into two decoupled subsystems. Ngamroo and Tippayachai [9] developed a robust decentralized frequency stabilizers design of SSSC by taking system uncertainties into consideration and proposed to use a SSSC in an interconnected power system which was subjected to load disturbances with frequency variation in the vicinity of the inter-area oscillation mode. In [10], stability analysis and design of the SSSC controller based on modal analysis, nonlinear simulations, pole placement techniques and time and frequency response techniques are investigated. In [11], PID structures are proposed to modulate the injected voltage through differential evolution algorithm. In [6], the authors propose a 12-pulse based SSSC with and without superconducting magnetic energy storage for enhancing the voltage stability and power oscillation damping in multi area system.

These proposals are based on small disturbance analysis that requires linearization of the system involved. However, linear methods cannot properly capture complex dynamics of the system,

* Corresponding author. Tel.: +237 77 59 52 19.
*E-mail addresses:* nguimfackjdedieu@yahoo.fr (J.d.D. Nguimfack-Ndongmo), gokenne@yahoo.com (G. Kenné), kuate_rf@yahoo.fr (R. Kuate-Fochie), acheuk_fr@yahoo.fr (A. Cheukem), hbfotsin@yahoo.fr (H.B. Fotsin), lamnabhi@lss.supelec.fr (F. Lamnabhi-Lagarrigue).

0142-0615/$ - see front matter © 2013 Elsevier Ltd. All rights reserved.
http://dx.doi.org/10.1016/j.ijepes.2013.08.019

especially during major disturbances. In [12,13], the authors proposed nonlinear control law based on Lyapunov stability concept to determine the additional damping provided by Controllable Series Capacitor (CSC). However, the time-derivative of the signals used in the control law are obtained by using band-pass filters and the problem of noise is not completely solve. The Lyapunov's stability theory have also been used to design a control law for SSSC in [14,15]. But in these contributions the formulation of the proposed control in the case of multimachine configuration has not been investigated.

Given that wind power is becoming increasingly significant source of energy, many power systems contain nowadays both synchronous generators (SGs) and doubly fed induction generators (DFIGs). It is known that a DFIG can contribute to stabilize a power system when it is subjected to small perturbations [16]. To the best of our knowledge, the impact of DFIG after large disturbances has not been investigated in multimachine power systems with the presence of FACTS device.

### 1.2. Main contribution

A simplified nonlinear method is proposed to enhance the transient stability of multimachine power system using SSSC device by exploiting the concepts developed in [12,13]. A new nonlinear control scheme has been derived and the time-derivative signals used in the proposed control scheme has been estimated in finite time by using second order sliding mode observers. The impact of DFIGs after large disturbances with the presence of FACTS device in multimachine power system has been investigated.

### 1.3. Structure of the paper

The paper is organized as follows. In Section 2, the injection model of the SSSC is described. The design procedure of the formulation of the proposed control algorithm is presented in Section 3. Simulation results are presented in Section 4 to demonstrate the performance of the proposed controller. Finally, in Section 5, some concluding remarks end the paper.

## 2. Modeling of the SSSC

The SSSC consists of a boosting transformer with a leakage reactance $X_{se}$, a three phase GTO based voltage source converter (VSC) and a DC capacitor $C$. The SSSC can be modeled as AC source $V_{se}\angle\theta_{se}$ [17]. $\theta_{se}$ is the phase of the injected voltage and is kept in quadrature with the line current ($I_l\angle\theta_c$) assuming that inverter losses are ignored. Therefore, the compensation level of the SSSC can be controlled dynamically by changing the injected voltage. Hence, if the SSSC is equipped with a damping controller, it can effectively improve power system dynamic stability.

### 2.1. VSC dynamic model

In the time scale of transient stability, in which the switching dynamics are neglected, the model of a VSC with the modulation ratio $m$ and the firing angle $\theta_{se}$ is given as follows [18]:

$$\underline{V}_{se} = mkV_{dc}(\cos\theta_{se} + j\sin\theta_{se}), \tag{1}$$

$$\underline{I}_l = I_{ld} + jI_{lq}, \tag{2}$$

$$\dot{V}_{dc} = \frac{mk}{C_{dc}}(I_{ld}\cos\theta_{se} + I_{lq}\sin\theta_{se}), \tag{3}$$

where $k$ is the fixed ratio between the VSC and DC voltage. During transient periods, the DC link capacitor exchange energy with the system and this is described by the dynamical Eq. (3).

### 2.2. SSSC unit insertion into a power system line

If a SSSC unit is inserted into a line between bus $l$ and bus $k$ (see Fig. 1) characterized by the reactance $X_{lk}$, the voltages $\underline{V}_l$ and $\underline{V}_k$ and the current $\underline{I}_{lk}$ are related as follows:

$$\underline{V}_l = V_{se}e^{j\theta_{se}} - j(X_{lk} + X_{se})\underline{I}_{lk} + \underline{V}_k. \tag{4}$$

The series voltage source can then be transformed to Norton equivalent having current $\underline{I}_{se} = \frac{\underline{V}_{se}}{j(X_{lk}+X_{se})}$ as shown in Fig. 1:

The transformed series voltage source enables the introduction of bus power injections into buses as shown in Fig. 2 (see [19,20]). The injections are obtained using the current $\underline{I}_{se}$ and the bus voltages $V_l\angle\theta_l$ and $V_k\angle\theta_k$ as:

$$\underline{S}_{lse} = \underline{V}_l\underline{I}^*_{se} = P_{lse} + jQ_{lse} \tag{5}$$

$$\underline{S}_{kse} = \underline{V}_k(-\underline{I}^*_{se}) = P_{kse} + jQ_{kse} \tag{6}$$

where

$$P_{lse} + jQ_{lse} = \frac{V_lV_{se}}{X_{lk}+X_{se}}[-\sin(\theta_l - \theta_{se}) + j\cos(\theta_l - \theta_{se})]$$

$$P_{kse} + jQ_{kse} = \frac{V_kV_{se}}{X_{lk}+X_{se}}[\sin(\theta_k - \theta_{se}) - j\cos(\theta_k - \theta_{se})]$$

## 3. Design procedure of nonlinear controller for SSSC in multimachine power systems

Direct Lyapunov method is a powerful tool for transient stability assessment and control of power systems. This method has been used in [12,13,21,22] for the design of damping controllers. In the following analysis, the Lyapunov theory is used to design an additional damping nonlinear controller in order to improve power system transient stability.

### 3.1. Concept of Lyapunov's stability theory

Let us consider the following nonlinear system

$$\dot{x} = F(x), \tag{7}$$

where $x$ is the vector of the state variables. The state $x_e$ is the equilibrium point of the dynamic system (e.g. $F(x_e) = 0$). Lyapunov's stability theorem states that this equilibrium point is asymptotically stable if there exists a Lyapunov function $\vartheta(x)$ such that $\vartheta(x)$ is positive definite with a minimum value at the equilibrium point $x_e$ and the time derivative $\dot{\vartheta}(x)$ along the system trajectory $x(t)$ is negative.

### 3.2. Multimachine power system model

Consider a power network which is modeled by $2n + N$ nodes connected by lossless transmission lines which is represented by node admittance matrix $\underline{Y} = j[B_{kl}]$. The first n nodes are the internal buses of the generators. The nodes $n + 1$ to $2n$ are the terminal buses of the generators. The remaining N nodes are the load buses. For the nodes $k = n + 1$ to $k = 2n + N$, the bus voltage is described by $V_k\angle\theta_k$.

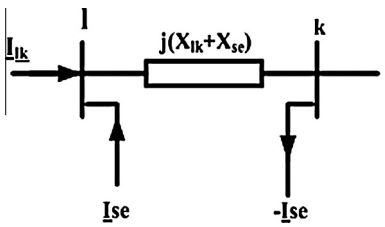


**Fig. 1.** Current source model of SSSC.

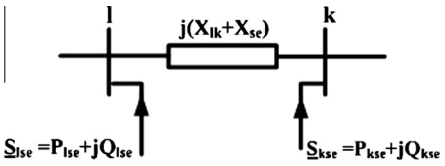


**Fig. 2.** Injection model of SSSC.

Each generator $k$ is described by some parameters: $\delta_k$ is the power angle of the generator which is valid over the region defined by $0 < \delta_k < \pi$; $\omega_k$ is the generator rotor angular speed; $M_k$ is the moment of inertia; $D_k$ is the damping coefficient; $x_{dk}$ is the direct axis reactance; $x'_{dk}$ is the generator transient reactance; $E_{fdk}$ is the equivalent EMF in the excitation coil; $T'_{d0k}$ is the direct axis transient open circuit time constant; $P_{mk}$ is the mechanical input power and $P_{ek}$ is the active power delivered to the terminal bus.

The center of inertia (COI) for the whole system $\delta_0$ and the center of speed $\omega_0$ are defined by [23]:

$$\delta_0 = \frac{1}{M_T}\sum_{k=1}^{n} M_k\delta_k \tag{8}$$

$$\omega_0 = \frac{1}{M_T}\sum_{k=1}^{n} M_k\omega_k \quad \text{where } M_T = \sum_{k=1}^{n} M_k. \tag{9}$$

The variables $\delta_k$, $\omega_k$ and $\theta_k$ are then transform to the COI variables as: $\tilde{\delta}_k = \delta_k - \delta_0$, $\tilde{\omega}_k = \omega_k - \omega_0$ and $\tilde{\theta}_k = \theta_k - \delta_0$.

The dynamics of the synchronous generators are described by the following differential equations with respect to the COI reference frame [12].

For $k = 1 \cdots n$,

$$\begin{aligned}
&\dot{\tilde{\delta}}_k = \tilde{\omega}_k,\\
&M_k\dot{\tilde{\omega}}_k = P_{m_k} - P_{ek} - D_k\tilde{\omega}_k - \frac{M_k}{M_T}P_{COI},\\
&T'_{d0_k}\dot{E}'_{q_k} = E_{fd_k} - \frac{x_{dk}}{x'_{dk}}E'_{q_k} + \frac{x_{dk}-x'_{dk}}{x_{dk}}V_{k+n}\cos(\delta_k - \theta_{k+n}),
\end{aligned} \tag{10}$$

where

$$P_{COI} = \sum_{k=1}^{n}(P_{m_k} - P_{ek}).$$

It is assumed that the mechanical input power of the generator is constant. The machine model considered here is flux-decay model (one-axis model). Exciters and governors are not included in this model.

For the lossless system, the following equations can be written at bus $k$ where $P_k$ is the real power and $Q_k$ is the reactive power injected into the system from bus k.

For $k = (2n+1) \cdots (2n+N)$,

$$\begin{aligned}
P_k &= \sum_{l=n+1}^{2n+N} B_{kl}V_kV_l\sin(\theta_k - \theta_l),\\
Q_k &= -\sum_{l=n+1}^{2n+N} B_{kl}V_kV_l\cos(\theta_k - \theta_l).
\end{aligned}$$

For $k = (n+1) \cdots 2n$,$P_k$ and $Q_k$ are similar, but also take account of generated real and reactive power [12,13,23].

Real load at each bus is represented by a constant active load and reactive load by an arbitrary function of voltage at the respective bus.

Thus, for $k = (n+1) \cdots (2n+N)$,

$$\begin{aligned}
P_{Lk} &= P^0_{Lk},\\
Q_{Lk} &= f_{qk}(V_k)
\end{aligned}$$

### 3.3. Design of control Lyapunov function for SSSC

An energy function for the differential algebraic (10) is given by [24,13]:

$$\vartheta\left(\tilde{\omega},\tilde{\delta},E'_q,V,\tilde{\theta}\right) = \vartheta_1 + \sum_{k=1}^{8}\vartheta_{2k} + \vartheta_0 \tag{11}$$

where

$$\vartheta_1 = \frac{1}{2}\sum_{k=1}^{n} M_k\tilde{\omega}_k^2, \quad \vartheta_{12} = -\sum_{k=1}^{n} P_{mk}\tilde{\delta}_k$$

$$\vartheta_{22} = \sum_{k=n+1}^{2n+N} P_{Lk}\tilde{\theta}_k, \quad \vartheta_{23} = \sum_{k=n+1}^{2n+N}\int\frac{Q_{Lk}}{V_k}dV_k$$

$$\vartheta_{24} = \sum_{k=n+1}^{2n}\frac{1}{2x'_{dk-n}}\left[E'^2_{qk-n} + V_k^2 - 2E'_{qk-n}V_k\cos(\tilde{\delta}_{k-n} - \tilde{\theta}_k)\right]$$

$$\vartheta_{25} = -\frac{1}{2}\sum_{k=n+1}^{2n+N}\sum_{l=n+1}^{2n+N} B_{kl}V_kV_l\cos(\tilde{\theta}_k - \tilde{\theta}_l)$$

$$\vartheta_{26} = \sum_{k=n+1}^{2n}\frac{x'_{dk-n} - x_{qk-n}}{4x'_{dk-n}x_{qk-n}}\left[V_k^2 - V_k^2\cos(2(\tilde{\delta}_{k-n} - \tilde{\theta}_k))\right]$$

$$\vartheta_{27} = -\sum_{k=1}^{n}\frac{E_{fdk}E'_{qk}}{x_{dk} - x'_{dk}}, \quad \vartheta_{28} = \sum_{k=1}^{n}\frac{E'^2_{qk}}{2(x_{dk} - x'_{dk})}.$$

$\vartheta_1$ is known as the kinetic energy and $\sum\vartheta_{2k}$ as the potential energy. $\vartheta_0$ is the constant such that at the post-fault stable equilibrium point, the energy function is zero.

Using the notation $\left[\frac{d\vartheta}{dt}\right]_{\dot{\omega}}$ for $\frac{\partial\vartheta}{\partial t}\frac{d\dot{\omega}}{dt}$, and similarly for the other states, we have:

$$\left[\frac{d\vartheta_1}{dt}\right]_{\dot{\omega}} + \left[\frac{d\vartheta_{21}}{dt} + \frac{d\vartheta_{24}}{dt} + \frac{d\vartheta_{26}}{dt}\right]_{\dot{\delta}} = -\sum_{k=1}^{n} D_k\tilde{\omega}_k^2 \tag{12}$$

$$\left[\frac{d\vartheta_{22}}{dt} + \frac{d\vartheta_{24}}{dt} + \frac{d\vartheta_{25}}{dt} + \frac{d\vartheta_{26}}{dt}\right]_{\dot{\theta}} = \sum(P_k + P_{Lk})\dot{\tilde{\theta}}_k = 0 \tag{13}$$

$$\left[\frac{d\vartheta_{23}}{dt} + \frac{d\vartheta_{24}}{dt} + \frac{d\vartheta_{25}}{dt} + \frac{d\vartheta_{26}}{dt}\right]_{V} = \sum(Q_k + Q_{Lk})\frac{\dot{V}_k}{V_k} = 0 \tag{14}$$

$$\left[\frac{d\vartheta_{27}}{dt} + \frac{d\vartheta_{28}}{dt} + \frac{d\vartheta_{24}}{dt}\right]_{E'_q} = -\sum_{k=1}^{n}\frac{T_{d0k}}{x_{dk} - x'_{dk}}E'^2_{qk} \tag{15}$$

The time derivative of the energy function without SSSC is given by:

$$\dot{\vartheta}_{no_{sssc}} = -\sum_{k=1}^{n} D_k\tilde{\omega}_k^2 - \sum_{k=1}^{n}\frac{T_{d0k}}{x_{dk} - x'_{dk}}E'^2_{qk} \leqslant 0 \tag{16}$$

The introduction of the SSSC does not alter the energy function (11). However, it does alter $\dot{\vartheta}$. The sums (13) and (14) no longer equal to zero. To prove this, let's consider the $k$-th term of (13). Without the SSSC connected to bus k, $(P_k + P_{Lk})\dot{\tilde{\theta}}_k = 0$. When the SSSC is connected, the power balance gives $(P_k + P_{Lk} + P_{kse}) = 0$. Therefore, the $k$-th term of (13) becomes $(P_k + P_{Lk})\dot{\tilde{\theta}}_k = -P_{kse}\dot{\tilde{\theta}}_k$. A similar argument is given for the $l$-th term of (13) and for the corresponding terms of (14). Then, with the SSSC connected between bus $l$ and bus k, (13) and (14) are modified, resulting in (17) and (18) as:

$$\left[\frac{d\vartheta_{22}}{dt} + \frac{d\vartheta_{24}}{dt} + \frac{d\vartheta_{25}}{dt} + \frac{d\vartheta_{26}}{dt}\right]_{\dot{\theta}} = -P_{lse}\dot{\tilde{\theta}}_l - P_{kse}\dot{\tilde{\theta}}_k. \tag{17}$$

$$\left[\frac{d\vartheta_{23}}{dt} + \frac{d\vartheta_{24}}{dt} + \frac{d\vartheta_{25}}{dt} + \frac{d\vartheta_{26}}{dt}\right]_{V} = -Q_{lse}\frac{\dot{V}_l}{V_l} - Q_{kse}\frac{\dot{V}_k}{V_k}. \tag{18}$$

where

$$P_{lse} = -\frac{V_l V_{se}}{X_{lk}+X_{se}}\sin(\theta_l-\theta_{se}),$$
$$Q_{lse} = \frac{V_l V_{se}}{X_{lk}+X_{se}}\cos(\theta_l-\theta_{se}),$$
$$P_{kse} = \frac{V_k V_{se}}{X_{lk}+X_{se}}\sin(\theta_k-\theta_{se}),$$
$$Q_{kse} = -\frac{V_k V_{se}}{X_{lk}+X_{se}}\cos(\theta_k-\theta_{se}).$$

Since $P_{lse} = -P_{kse}$ for the SSSC and all control series devices, the time derivative of the energy function becomes:

$$\dot{\vartheta} = -\sum_{k=1}^{n} D_k\tilde{\omega}_k^2 - \sum_{k=1}^{n}\frac{T_{d0k}}{x_{dk}-x'_{dk}}E'^2_{qk} - P_{lse}(\dot{\tilde{\theta}}_l-\dot{\tilde{\theta}}_k) - Q_{lse}\frac{\dot{V}_l}{V_l} - Q_{kse}\frac{\dot{V}_k}{V_k} \quad (19)$$

$$= \dot{\vartheta}_{no_{sssc}} + \dot{\vartheta}_{sssc}. \quad (20)$$

with

$$\dot{\vartheta}_{sssc} = -\left[P_{lse}(\dot{\tilde{\theta}}_l-\dot{\tilde{\theta}}_k) + Q_{lse}\frac{\dot{V}_l}{V_l} + Q_{kse}\frac{\dot{V}_k}{V_k}\right] \quad (21)$$

$$= \frac{V_{se}V_l}{X_{lk}+X_{se}}\left[\dot{\tilde{\theta}}_{lk}\sin(\theta_l-\theta_{se}) - \frac{\dot{V}_l}{V_l}\cos(\theta_l-\theta_{se}) + \frac{\dot{V}_k}{V_l}\cos(\theta_k-\theta_{se})\right], \quad (22)$$

where $\theta_{lk} = \theta_l - \theta_k, \dot{\tilde{\theta}}_{lk} = \dot{\tilde{\theta}}_l - \dot{\tilde{\theta}}_k$.

Since the angle of the injected voltage $\theta_{se}$ is kept in quadrature with the current ($I_{lk}$) through the SSSC,

let $\theta_{se} = \theta_c + \gamma$ with $\gamma = \pm\frac{\pi}{2}$ and $\theta_c$ the angle of this current. Then (22) becomes:

$$\dot{\vartheta}_{sssc} = -\frac{V_{se}V_l\sin\gamma}{X_{lk}+X_{se}}\left[\omega_{lk}\cos\theta_{lc} + \frac{\dot{V}_l}{V_l}\sin\theta_{lc} - \frac{\dot{V}_k}{V_l}\sin\theta_{kc}\right]. \quad (23)$$

where

$$\theta_{lc} = \theta_l - \theta_c,$$
$$\theta_{kc} = \theta_k - \theta_c,$$
$$\omega_{lk} = \dot{\tilde{\theta}}_{lk} = \dot{\theta}_{lk}.$$

The SSSC device contributes to the system damping if $\dot{\vartheta}_{sssc}$ is negative. In order to achieve this objective, let ($K > 0$ is a design parameter and its value depend on the rating of the SSSC):

$$V_{se} = K\omega_{lk}^2 V_l, \quad 0 \leqslant V_{se} \leqslant V_{se}^{max}; \quad (24)$$

$$\sin\gamma = \text{sign}\left[\omega_{lk}\cos\theta_{lc} + \frac{\dot{V}_l}{V_l}\sin\theta_{lc} - \frac{\dot{V}_k}{V_l}\sin\theta_{kc}\right]. \quad (25)$$

By choosing $V_{se}$ and $\sin\gamma$ as given by (24) and (25), (20) becomes:

$$\dot{\vartheta} = -\sum_{k=1}^{n} D_k\tilde{\omega}_k^2 - \sum_{k=1}^{n}\frac{T_{d0k}}{x_{dk}-x'_{dk}}E'^2_{qk} - \frac{K\omega_{lk}^2V_l^2}{X_{lk}+X_{se}}\left|\omega_{lk}\cos\theta_{lc}, + \frac{\dot{V}_l}{V_l}\sin\theta_{lc} - \frac{\dot{V}_k}{V_l}\sin\theta_{kc}\right|$$

$$\Rightarrow \dot{\vartheta} \leqslant 0. \quad (26)$$

This means that the introduction of the SSSC controlled by (24) and (25) provides additional damping of the power system.

Remarks:

(i) The above control law relies only on locally measurable information and is independent of system topology and modeling of power system components.

The proposed control scheme is implementable in real-time since it needs only measurable signals ($V_i$ $i = l, k$; $\theta_{lk}$) which can be obtained using phasor measurements [12].

(ii) The control law is in the form of pure derivatives. The time-derivatives of $V_l$, $V_k$ and $\theta_{lk}$ cannot be obtained directly using numerical differentiation due to the presence of noise. In [13] band-pass filters tuned at the frequency range of interest have been used to avoid adverse action of the controller of a CSC. However, the problem of noise is not completely solve in this method. To overcome this problem, second order sliding mode observers must be used to estimate the above unavailable states in finite time in Section 3.4.

### 3.4. State observers design

To estimate the unavailable time-derivative signals required for the implementation of the above controller, let us introduce the following variables:

$$x_{i1} = V_i;$$
$$\dot{x}_{i1} = x_{i2} = \dot{V}_i, \quad i = l, k; \quad (27)$$
$$u_{lk1} = \theta_{lk};$$
$$\dot{u}_{lk1} = u_{lk2} = \dot{\theta}_{lk}. \quad (28)$$

The following assumption will be considered until further notice:

(i) The signals ($V_i$, $i = l, k$; $\theta_{lk}$) are assumed to be continuous and bounded.

Let us consider now the following second-order sliding mode observers [25,26]:

$$\dot{\hat{x}}_{i1} = \hat{x}_{i2} + z^1_{x_i}, \quad i = l, k; \quad (29)$$
$$\dot{\hat{x}}_{i2} = z^2_{x_i}.$$
$$\dot{\hat{u}}_{lk1} = \hat{u}_{lk2} + z^1_{u_{lk}}; \quad (30)$$
$$\dot{\hat{u}}_{lk2} = z^2_{u_{lk}}.$$

where the variables $z^1_{x_i}, z^2_{x_i}$, $z^1_{u_{lk}}$ and $z^2_{u_{lk}}$ are given by the following expressions:

$$z^1_{x_i} = -\beta_{x_i}|\hat{x}_{i1} - x_{i1}|^{1/2}\text{sign}(\hat{x}_{i1} - x_{i1}), \quad (31)$$
$$z^2_{x_i} = -\alpha_{x_i}\text{sign}(\hat{x}_{i1} - x_{i1}),$$
$$z^1_{u_{lk}} = -\beta_{u_{lk}}|\hat{u}_{lk1} - u_{lk1}|^{1/2}\text{sign}(\hat{u}_{lk1} - u_{lk1}), \quad (32)$$
$$z^2_{u_{lk}} = -\alpha_{u_{lk}}\text{sign}(\hat{u}_{lk1} - u_{lk1}).$$

and $\alpha_{x_i}, \beta_{x_i}, \alpha_{u_{lk}}, \beta_{u_{lk}}$ are positive tuning parameters. The solutions of the above observers are understood in the Filippov sense [25]. Taking $e_{x_{i1}} = \hat{x}_{i1} - x_{i1}$, $e_{x_{i2}} = \hat{x}_{i2} - x_{i2}$, $e_{u_{lk1}} = \hat{u}_{lk1} - x_{lk1}$, $e_{u_{lk2}} = \hat{u}_{lk2} - u_{lk2}$, the following dynamics errors equations are obtained:

$$\dot{e}_{x_{i1}} = e_{x_{i1}} - \beta_{x_1}|e_{x_{i1}}|^{1/2}\text{sign}(e_{x_{i1}}), \quad (33)$$
$$\dot{e}_{x_{i2}} = -x_{i2} - \alpha_{x_{i1}}\text{sign}(e_{x_{i1}}),$$
$$\dot{e}_{u_{lk1}} = e_{u_{lk1}} - \beta_{u_{lk1}}|e_{u_{lk1}}|^{1/2}\text{sign}(e_{u_{lk1}}), \quad (34)$$
$$\dot{e}_{x_{lk2}} = -u_{lk2} - \alpha_{u_{lk1}}\text{sign}(e_{ulk1}). \quad (35)$$

Assuming that the states of the system is bounded as reported in assumption (i) then there exists positive constants $\mu_{x_{i2}}$ and $\mu_{u_{lk2}}$ such that the inequalities

$$|x_{i2}| < \mu_{x_{i2}} \quad (36)$$
$$|u_{lk2}| < \mu_{u_{lk2}} \quad (37)$$

hold $\forall t, x_{i1}, x_{i2}, u_{lk1}$ and $u_{lk2}$. Then the variables of the observers converge to the states of the nonlinear reference model.

The proof of the finite time convergence of the estimated states to the real states can be found in [25].

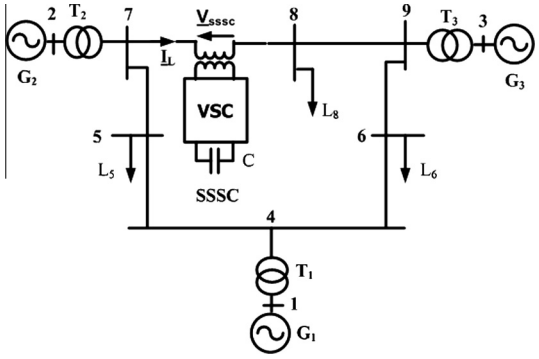


**Fig. 3.** WSCC system with SSSC.

### 3.5. Global convergence analysis

To achieve the global convergence and stability analysis, let us recall the nonlinear controller (24) and (25):

$$V_{se} = K\omega_{lk}^2 V_l, \quad 0 \leqslant V_{se} \leqslant V_{se}^{max} \tag{38}$$

$$\sin\gamma = \text{sign}\left[\omega_{lk}\cos\theta_{lc} + \frac{\dot{V}_l}{V_l}\sin\theta_{lc} - \frac{\dot{V}_k}{V_l}\sin\theta_{kc}\right] \tag{39}$$

It has been proved in Section 3.3 that the introduction of the SSSC using the above non-adaptive controller provides additional damping of the power system.

In practice, the adaptive controller is used because the time-derivative signals required for the implementation of this control are not available. In this case, these time-derivative signals are substituted in the above non-adaptive controller by their estimates. Therefore, the adaptive controller is given by:

$$V_{se} = K\hat{u}_{lk2}^2 V_l, \quad 0 \leqslant V_{se} \leqslant V_{se}^{max} \tag{40}$$

$$\sin\gamma = \text{sign}\left[\hat{u}_{lk2}\cos\theta_{lc} + \frac{\hat{x}_{l2}}{V_l}\sin\theta_{lc} - \frac{\hat{x}_{k2}}{V_l}\sin\theta_{kc}\right] \tag{41}$$

The global convergence and stability analysis taking into account the interconnections between the second order sliding observers (29) and (30) and the nonlinear controller (40) and (41) are based on the separation principle theorem. The finite-time convergence of the observers allows to design the observers and the nonlinear control law separately, i.e., the separation principle is satisfied [25,26]. The only requirement for its implementation is the boundedness of the states of the system (assumption (i) and inequalities (36) and (37)) in the operational domain.

## 4. Simulation results

The effectiveness of the proposed state-variable stabilizing control has been verified by numerical simulations within the Matlab/Simulink environment software. The configuration of the multimachine used is the nine-bus WSCC system shown in Fig. 3. This system consists of three generators located at buses 1–3. All generators are assumed to be equipped with turbine-governor and voltage regulator loops [27]. Bus 1 is considered as the slack bus. Buses 5, 6 and 8 are the load buses. Pi-models are used for the transmission lines. A SSSC device is inserted in the line between bus 7 and bus 8.

The large disturbances considered in this work are 200 ms three phase; 650 ms three phase and 500 ms single phase short-circuit faults. These faults are supposed to occur at the end of the line 4–6 (near bus 6).

The 200 ms three phase short-circuit fault has been conducted according to the following sequence:

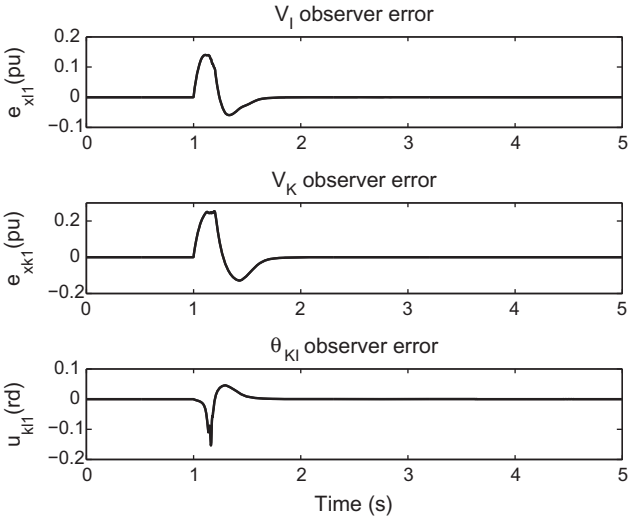


**Fig. 4.** Observer errors of the estimation of $V_l$, $V_k$, and $\theta_{lk}$ time-derivatives in case of 200 ms three phase short circuit.

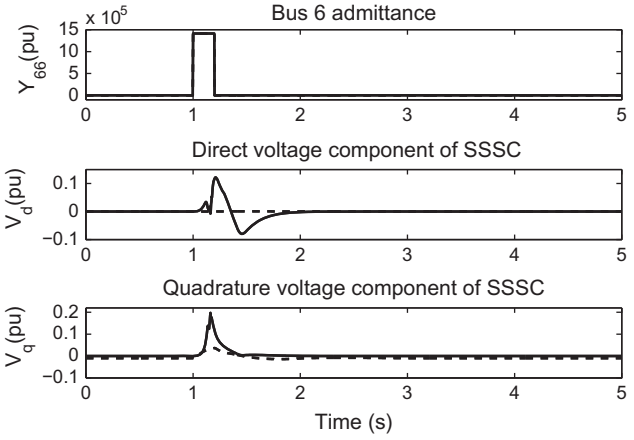


**Fig. 5.** Control voltage of SSSC in case of 200 ms three phase short circuit.

1. At $t = 0$, the system is in pre-fault state.
2. At $t = 1$ s, a three phase short-circuit fault occurs in the transmission lines.
3. At $t = 1.2$ s, the transmission line is restored and the system is in a post-fault state.

The 650 ms three phase short-circuit fault has been conducted according to the following sequence:

1. At $t = 0$, the system is in pre-fault state.
2. At $t = 1$ s, a three phase short-circuit fault occurs in the transmission lines.
3. At $t = 1.65$ s, the transmission line is restored and the system is in a post-fault state.

The single phase short-circuit fault has been carried out according to the following sequence:

1. At $t = 0$, the system is in pre-fault state.
2. At $t = 1$ s, a three phase short-circuit fault occurs in the transmission lines.
3. At $t = 1.5$ s, the transmission line is restored and the system is in a post-fault state.

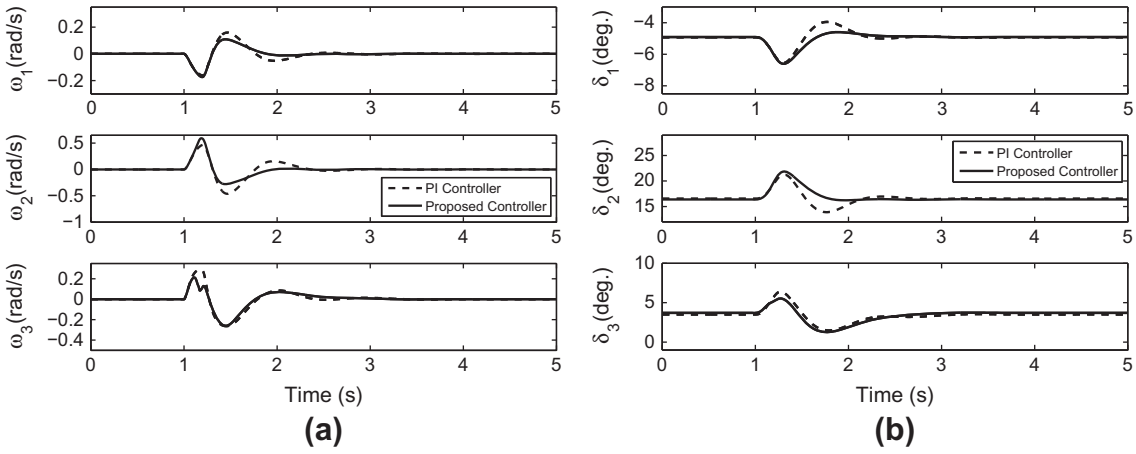


**Fig. 6.** Case of 200 ms three phase short circuit: (a) Relative speed of Generator 1, 2, 3. (b). Relative rotor angle of Generator 1, 2, 3.

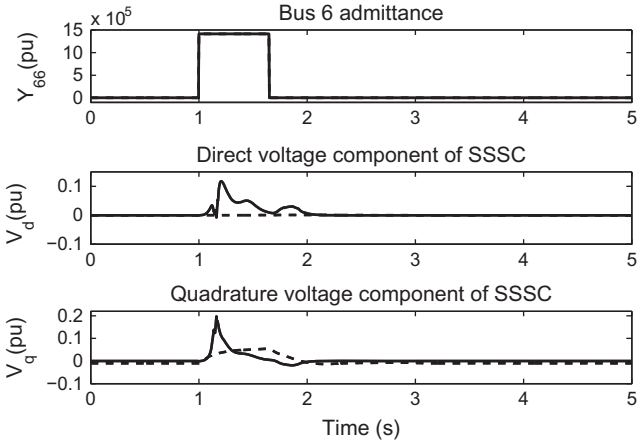


**Fig. 7.** Control voltage of SSSC in case of 650 ms three phase short circuit.

The tuning parameter used has been obtained by trial and error during multiple simulation tests and good results have been obtained for $K = 2$. For comparison, simulation results have been carrying out by using the conventional PI controller for SSSC.

The tuning parameters of the second order sliding mode observers (29) and (30) have been computed by using the guideline provided in [25] and these parameters are given in the appendix. The observer errors of the estimation of $V_l$, $V_k$, and $\theta_{lk}$ time-derivatives are shown in Fig. 4.

The comparative results for 200 ms three phase short circuit are documented in Figs. 5 and 6. In Fig. 7, Vq is the injected compensating control voltage. The SSSC performs the function of a variable reactance compensator, either capacitive ($Vq > 0$) or inductive ($Vq < 0$).

It can be noticed in Fig. 6 that the proposed method contribute to improve transient (first swing) and oscillation damping than the PI regulator. This is because, the conventional PI is linear controller, normally used to improve dynamic stability for small signals perturbations.

The comparative results for 650 ms three-phase short circuit are reported in Fig. 8.

The comparative results for 500 ms single-phase short circuit are reported in Fig. 9.

It can be noticed that the proposed method gives better performance than the PI controller.

In order to evaluate the impact of wind farm on the transient stability under large disturbance, generator 2 is replaced by the DFIG. The dynamics equations of the $i$th DFIG which take a similar form as those of the synchronous generator are [16,28]:

$$\begin{aligned}
\dot{\tilde{\delta}}_i &= \tilde{\omega}_i + \frac{x_{di} - x'_{di}}{x'_{di}} \frac{V_{i+n} \sin(\delta_i - \theta_{i+n})}{E'_{q_i} T'_{d0_i}} + \frac{\omega_s V_{ri} \cos(\delta_i - \theta_{ri})}{E'_{q_i}}, \\
M_i \dot{\tilde{\omega}}_i &= P_{m_i} - P_{ei} - D_i \tilde{\omega}_i - \frac{M_i}{M_T} P_{COI}, \\
T'_{d0_i} \dot{E}'_{q_i} &= T'_{d0_i} \omega_s V_{ri} \sin(\delta_i - \theta_{ri}) - \frac{x_{di}}{x'_{di}} E'_{q_i} + \frac{x_{di} - x'_{di}}{x_{di}} V_{i+n} \cos(\delta_i - \theta_{i+n}),
\end{aligned} \tag{42}$$

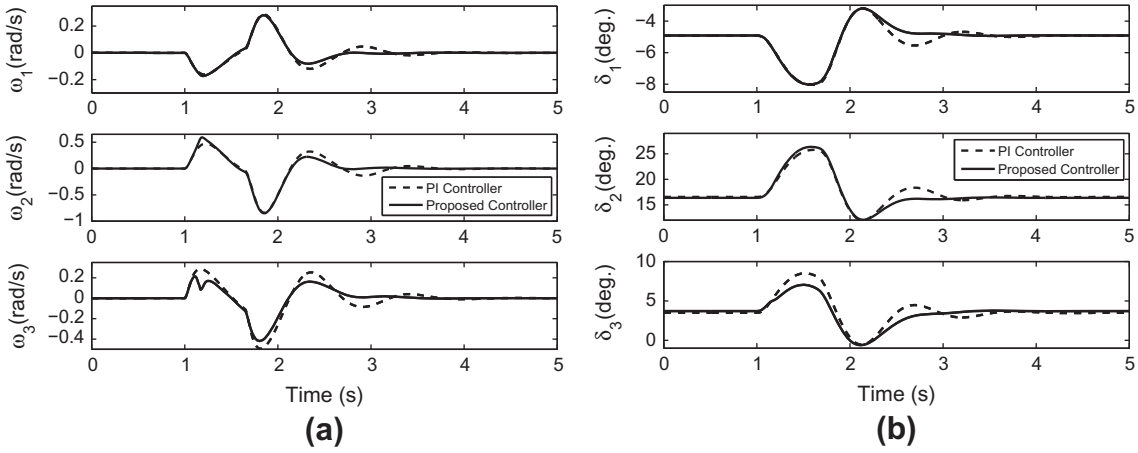


**Fig. 8.** Case of 650 ms three phase short circuit: (a) Relative speed of Generator 1, 2, 3. (b). Relative rotor angle of Generator 1, 2, 3.

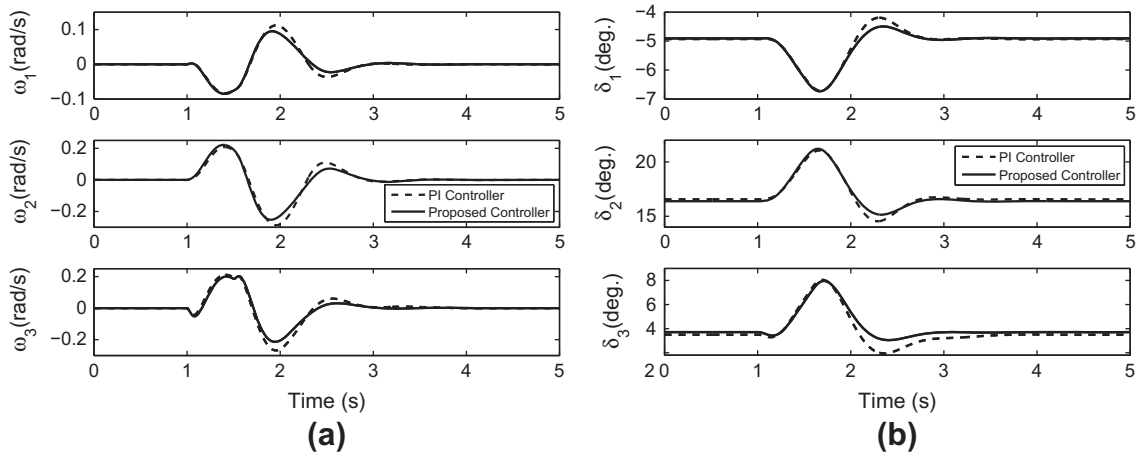


**Fig. 9.** Case of 500 ms single phase short circuit: (a) Relative speed of Generator 1, 2, 3. (b). Relative rotor angle of Generator 1, 2, 3.

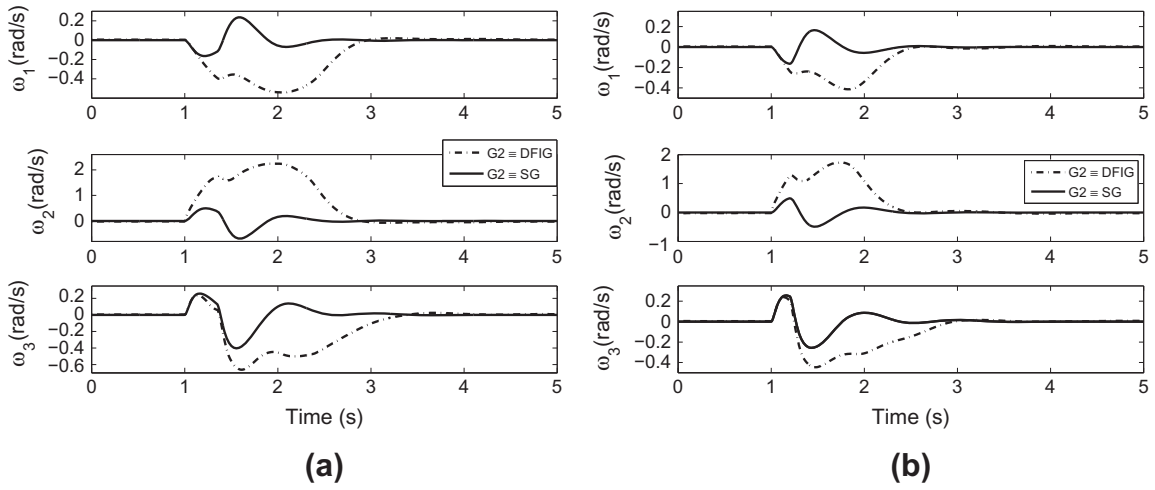


**Fig. 10.** Case of 200 ms three phase short circuit with G2 ≡ SG/DFIG: (a) Relative speed of Generator 1, 2, 3. (b) Relative rotor angle of Generator 1, 2, 3.

where $\omega_s$ is the synchronous speed and $V_{ri}\angle\theta_{ri}$ the rotor voltage of the $i$th DFIG.

The comparative results for 200 ms three phase short circuit in presence of DFIG are reported in Figs. 10 and 11. Fig. 10 shows that G2-SG has more effective action in transient stability than G2-DFIG, even in the presence of SSSC. The good performance in the presence of SG can be explained by the fact that there is no interruption of reactive power injected by G2 during the fault.

Fig. 11 shows that G2-SG injects ($Q_2 < 0$) reactive power during the fault while G2-DFIG consumes ($Q_2 > 0$) reactive power during the fault. This behavior explains the high magnitude value of oscillation during the fault and poor oscillation damping after fault clearance time.

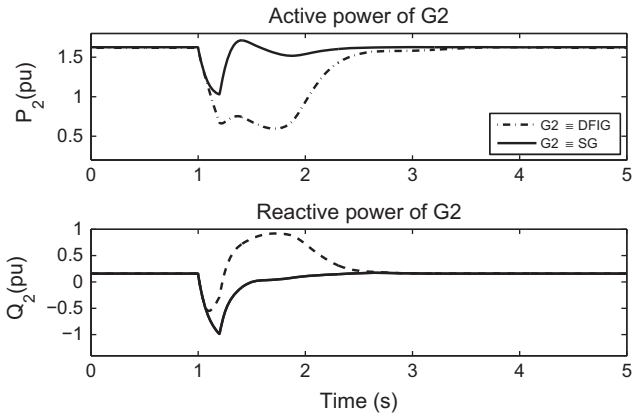


**Fig. 11.** Active power G2, reactive power G2 With G2 ≡ SG/DFIG.

## 5. Conclusion

In this paper, a simplified nonlinear method, suitable for transient stability enhancement of the multimachine power system using SSSC has been described. The proposed control law relies only on locally measurable information and is independent of system topology and modeling of power system components. The control scheme is implementable in real-time since it needs only measurable signals which can be obtained using phasor measurements. The simulation results show that the proposed nonlinear SSSC controller improves very satisfactorily the stability performance of the power system under severe disturbance operating conditions (200 ms, 650 ms three phase and 500 ms single phase short-circuit faults).

## Appendix A. System data and observers/PI-regulator parameters

The Generators data and initial operating points are taking from [29,23]:

| Parameter | $Gen_1$ | $Gen_2$ | $Gen_3$ |
|---|---|---|---|
| $H$ (s) | 23.64 | 6.40 | 3.01 |
| $X_d$ (pu) | 0.1460 | 0.8958 | 1.3125 |
| $x'_d$ (pu) | 0.0608 | 0.1198 | 0.1813 |
| $D$ (pu) | 0.3100 | 0.5305 | 0.6000 |
| $T'_{d0}$ (s) | 8.96 | 6.00 | 5.89 |
| $P_m$ (pu) | 0.7157 | 1.6295 | 0.8502 |
| $\delta_{ref}$ (deg) | 2.16 | 21.63 | 12.53 |
| $E'_{qref}$ (pu) | 1.0768 | 0.9833 | 1.0713 |

DFIG data are given as follows:

| $H$ (s) | $X_d$ (pu) | $x'_d$ (pu) | $D$ (pu) |
|---|---|---|---|
| 6.40 | 0.8958 | 0.1198 | 0.5350 |
| $T'_{d0}$ (s) | $\delta_{ref}$ (deg) | $E'_{qref}$ (pu) | $w_s$ (pu) |
| 01 | 21.63 | 0.9833 | 1 |

*SSSC*: $X_{se} = 0.12$ pu; $C = 2.26$ pu.
*State observers*: $\alpha_{x_i} = 2.55$; $\alpha_{u_{ik}} = 2.75$; $\beta_{u_{ik}} = 2.40$.

SSSC PI Controllers.

*DC voltage regulator*: $K_P = 5$; $K_I = 10$.
*Vq voltage regulator*: $K_P = 0.1$; $K_I = 9$.

## References


[1] Zangeneh A. A Lyapunov theory based UPFC controller for power flow controller. Electr Power Energy Syst 2009;31:302–8.
[2] Hingorani NG, Gyugyi L. Understanding FACTS concepts and technology of flexible AC transmission systems. New YorK: IEEE Press; 2000.
[3] Song Y, Johns T. Flexible AC transmission systems (FACTS). London: IEE; 2000.
[4] Yazdani A, Iravani R. Voltage sourced converters in powers systems. New Jersey: IEEE Press; 2010.
[5] Panda S. Modeling, simulation and optimal tuning of SSSC-based controller in a multimachine power system. World J Model Simulat 2010;6:110–21.
[6] Thangavel M, Scholar P, Jasmine S. Enhancement of voltage stability and power oscillation damping using static synchronous series compensator with smes. Int J Adv Res Technol 2012;2:94–8.
[7] Wang HF. Static synchronous series compensator to damp systems oscillations. Electric Power Syst Res 2000;54:113–9.
[8] Menniti D, Pinnarelli A, Scordino N, Nicola S. Using a FACTS device controlled by a decentralized control law to damp the transient frequency deviation in a deregulated electric power system. Electric Power Syst Res 2004;72:289–98.
[9] Ngamroo I, Tippayachai J. Robust decentralised frequency stabilizers design of static synchronous series compensators by taking system uncertainties into consideration. Electric Power Syst Res 2006;28:513–24.
[10] Castro MS, Ayres HM, Da Costa VF, Da Silva LPC. Impacts of the SSSC control modes on small-signal and transient stability of a power system. Electric Power Syst Res 2007;77:1–9.
[11] Swain S, Mahapatra S, Panda S. Design of the optimized sssc based facts controller. Int J Electron Electrical Eng 2012;2.
[12] Ghandhari M, Andersson G, Zanetta Al, Hiskens. Control Lyapunov functions for controllable series devices. IEEE Trans Power Syst 2001;16–4:689–94.
[13] Ghandhari M, Andersson G, Pavella M, Ernst D. A control strategy for controllable series capacitor in electric power systems. Automatica 2001;37:1575–83.
[14] Haque MH. Determination of additional damping provided by a SSSC through evaluation of rate dissipation of transient energy. In: 2004 International Conference on Power System Technology, (POWERCON'2004), vol. 2, Singapore; November 2004. p. 1942–1947.
[15] Haque MH. Damping improvement by facts devices: a comparison between statcom and SSSC. Electric Power Syst Res 2006;76:865–72.
[16] Elkington K, Knazkins V, Ghandhari M. On the stability of power systems containing doubly fed induction generator-based generation. Electric Power Syst Res 2008;78:1477–84.
[17] Jamali S, Shateri H. Locus of apparent impedance of distance protection in the presence of SSSC. Eur Trans Electrical Power 2010;21:398–412.
[18] Wang H. Static synchronous series compensator to damp power system oscillations. Electric Power Syst Res 2000;54:113–9.
[19] Xiao-Ping Z, Christian R, Biskash P. Flexible AC transmission systems: modelling and control. Germany: Springer; 2006.
[20] Dizdarevic N. Unified power flow controller in alleviation of voltage stability problem, Ph.D. dissertation. University of Zagreb Faculty of Electrical Engineering & Computing Department of Power Systems; 2001.
[21] Machowski J, Bialek J. State-variable control of shunt facts devices using phasor measurements. Electric Power Syst Res 2008;78:39–48.
[22] Caldon R, Mattavelli P, Han BM. Dynamic analysis and control of UPFC using transient simulation. In: International conference on power systems transients, Budapest, Hungary; 1999.
[23] Peter WS, Pai MA. Power system dynamics and stability. New Jersey: Prentice Hall; 1998.
[24] Pai MA. Energy function analysis for power system stability. Kluwer Academic Publishers; 1989.
[25] Levant A. Robust exact differentiation via sliding mode technique. Automatica 1998;34:379–84.
[26] Kenne G, Ahmed-Ali T, Lamnabhi-Lagarrigue F, Arzandé A. An improved rotor resistance estimator for induction motors adaptive control. Electric Power Syst Res 2011;81:930–41.
[27] Radman G, Raje RS. Dynamic model for power systems with multiple FACTS controllers. Electric Power Syst Res 2008;78:361–71.
[28] Kanchanaharuthai A, Chankong V, Loparo K. Small-signal stability enhancement of power systems with renewable energy resources. In: Preprints of the 18th IFAC world congress. Milano: International Federation of Automatic Control; 2011. p. 513–8.
[29] Colbia-Vegaa A, Leon-Morales JD, Fridman L, Salas-Pen O, Mata-Jimenez MT. Robust excitation control design using sliding-mode technique for multimachine power systems. Electric Power Syst Res 2008;78:1627–34.